Supporting Information for

Electrocatalytic Nitrogen Reduction to Ammonia by Atomically Precise Cu_6 Nanoclusters Supported on Graphene Oxide

Aamir Shehzad,[ab] Chaonan Cui,*[a] Ran Cheng,[ab] Zhixun Luo*[ab]

[a] State Key Laboratory for Structural Chemistry of Unstable and Stable Species, Institute of Chemistry, Chinese Academy of Sciences, Beijing 100190, China

[b] School of Chemistry, University of Chinese Academy of Sciences, Beijing 100049, China

* Corresponding authors. Emails: chncui@iccas.ac.cn (CC); zxluo@iccas.ac.cn (ZL).

S1. Materials and Materials

Chemicals. All chemicals are commercially available and used without further purification, including cupric (II) acetate [$Cu(OAC)_2$, 99%, Alfar Aesar], triphenylphosphine gold (I) chloride ($AuClPPh_3$, 98%, Acros Organic), 2-mercapto-5-n-propylpyrimidine ($SN_2C_7H_{10}$, SMPP, 98%, Alfar Aesar), sodium borohydride ($NaBH_4$, 98%, Acros Organics) and triethylamine (98%, Acros Organics). Various solvents comprising dichloromethane (DCM), methanol, n-hexane and ethanol were purchased from Beijing chemical reagent Co. Ltd.

Other chemicals including graphene oxide, KOH, NaOH, HCl, salicylic acid, sodium citrate, sodium hypochlorite (NaClO), sodium nitroferricyanide dihydrate ($C_5FeN_6Na_2O.2H_2O$), NH_4Cl, *p*-dimethylaminobenzaldehyde ($C_9H_{11}NO$), hydrazine monohydrate ($N_2H_4.H_2O$), Nafian D521 (5 wt%) were commercially purchased without further purification. The water used for the experiment was Milli-Q water, produced by a Millipore apparatus. The carbon paper electrode was used for preparation of working electrode.

Characterization. The UV-vis absorption spectra were collected using an UV-3600 Shimadzu UV-vis-NIR spectrophotometer. The single-crystal X-ray diffraction (XRD) data of the synthesized Cu_6 nanoclusters was measured on an Rigaku MM007HF Saturm724+ single crystal X-ray diffractometer with Mo Kα radiation (λ=0.71073 Å). The single crystal structure was solved by direct methods and refined with full-matrix-least-squares on F^2. High resolution of electrospray ionization time-of-flight mass spectrometry (ESI-TOF-MS) measurements was conducted by a Bruker Solarix 9.4T in the positive ionization mode. To clarify the surface atoms, present in the single crystal structure according to the crystal structure data and core-level binding energies (BEs) compared to their surface oxidation states, X-ray photoelectron spectroscopy (XPS) was collected by a Thermo Fisher Scientific EscaLab250Xi spectrometer. The high-resolution morphological features of GO-supported $Cu_6(SMPP)_6$ NCs were examined on high resolution transmission electron microscope (HRTEM) JSM200FS.

Quantification of hydrazine byproduct. Additionally, considering hydrazine to be a likely byproduct during dinitrogen reduction to ammonia, the quantification of hydrazine was also tested using the Watt and Chrisp method.[1] Hydrazine reacts with p-dimethylaminobenzaldehyde (PDABA, $C_9H_{11}NO$) in acidic media to generate yellow products with a UV-vis absorption band at 455 nm, which is used for hydrazine determination spectrophotometrically. A mixed solution of 30 mL volume of HCl (1 M), 300 mL anhydrous ethanol and 5.99 g PDABA was used as a colour reagent in this study. The standard reference solutions based on $N_2H_4 \cdot H_2O$ (85 %) were prepared with the concentrations of 0, 0.1, 0.2, 0.3, 0.4, 0.5, and 0.6 $\mu g \cdot mL^{-1}$ to plot the calibration curve. Later, 5 mL volume of colour reagent and 5 mL volume of the reference solution were added to the ENRR sample solutions. After 15 minutes, absorbance at 457 nm was recorded. From the UV-vis absorption for N_2H_4 standard solutions, the obtained calibration curve $y=1.290x-0.00379$ ($R^2=0.999$) shows a good linear relation of absorbance values with hydrazine concentrations. The yield of hydrazine after each ENRR test was evaluated by mixing 5 mL colour reagent with 5 mL residual electrolyte, and UV-vis absorption spectra were also recorded after incubation for 15 minutes.

Fig. S1 ENRR working Apparatus (a) H-cell (b) Electrochemical workstation CHI660E.

S2. Experimental Details

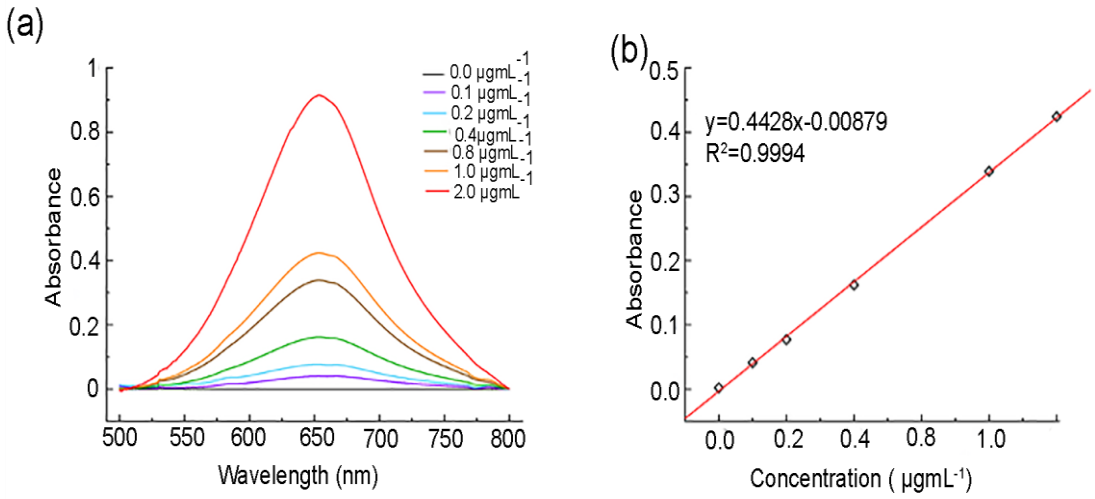

Fig. S2 (a) UV-vis absorption spectra of indophenol assays with NH_4^+ ions after incubation for 2 hours at room temperature in dark conditions. (b) Calibration curve used for determination of NH_3 concentration.

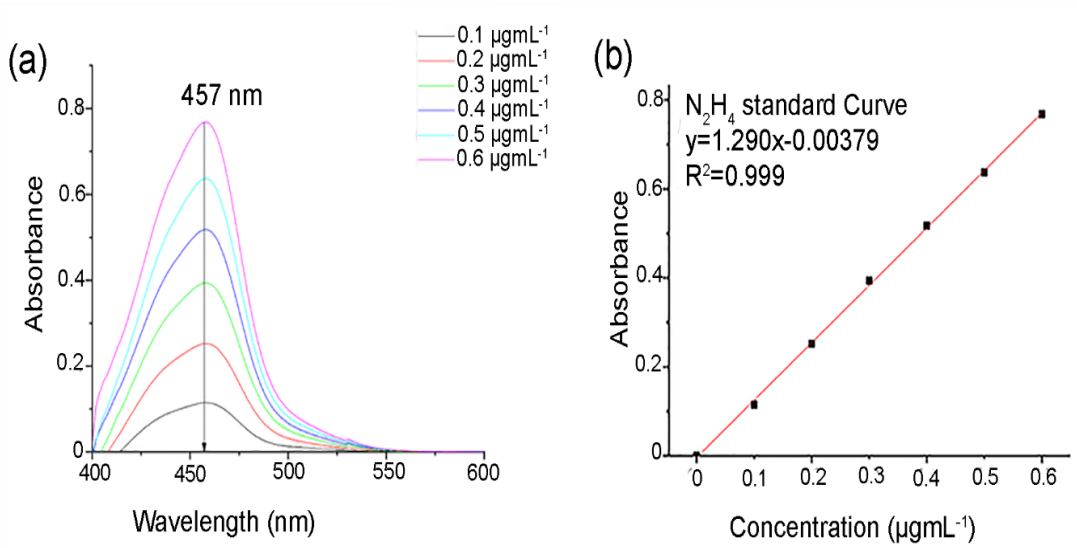

Fig. S3 (a) UV-vis absorption spectra for N_2H_4 standard solutions with different concentrations. (b) Calibration curve used for estimation of N_2H_4 concentration.

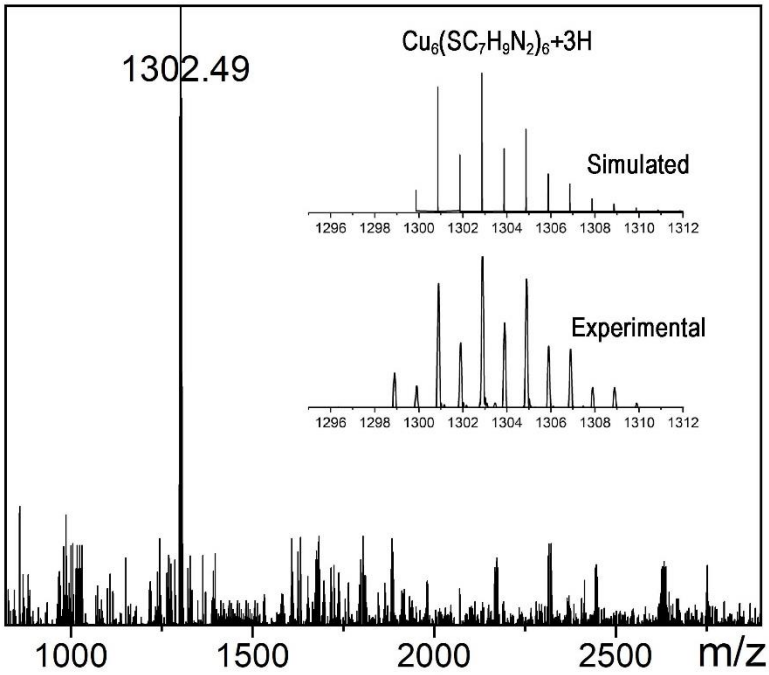

Fig. S4 ESI-MS experimental spectrum of synthesized $Cu_6(SMPP)_6$ nanoclusters in the positive mode.

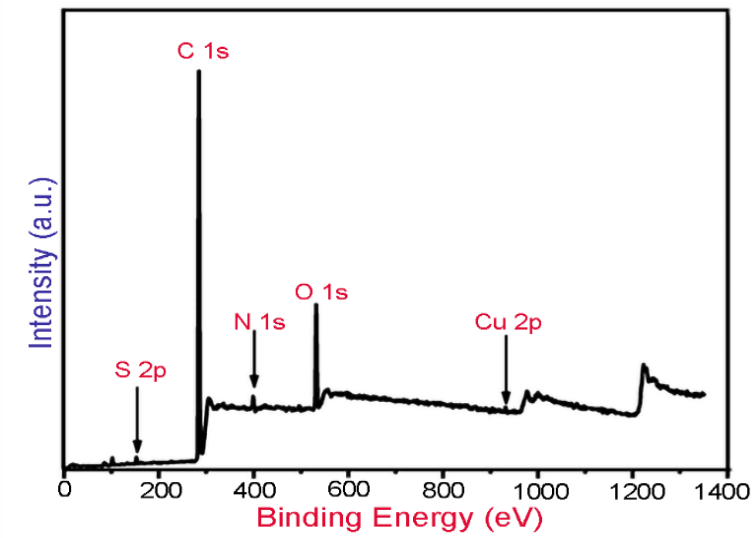

Fig. S5 Full survey XPS spectrum of the $Cu_6(SMPP)_6$ nanoclusters.

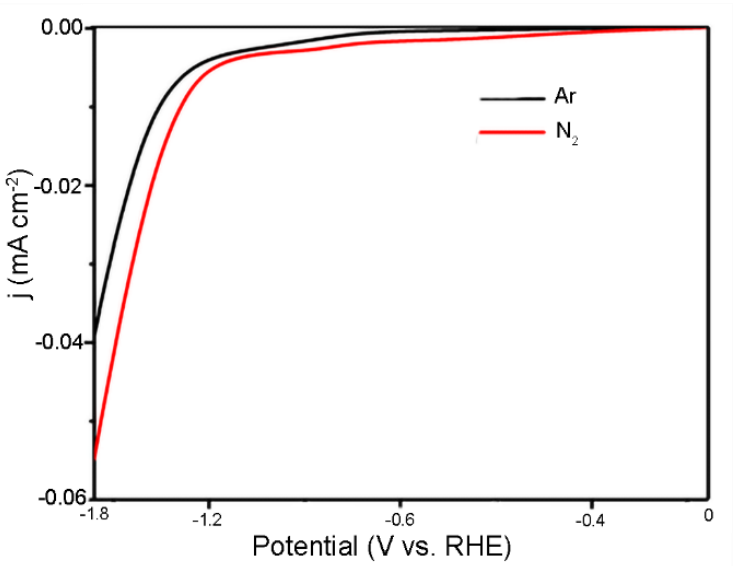

Fig. S6 LSV curve for unsupported Cu_6 nanoclusters in N_2 and Ar-saturated 0.1 M KOH electrolyte solution.

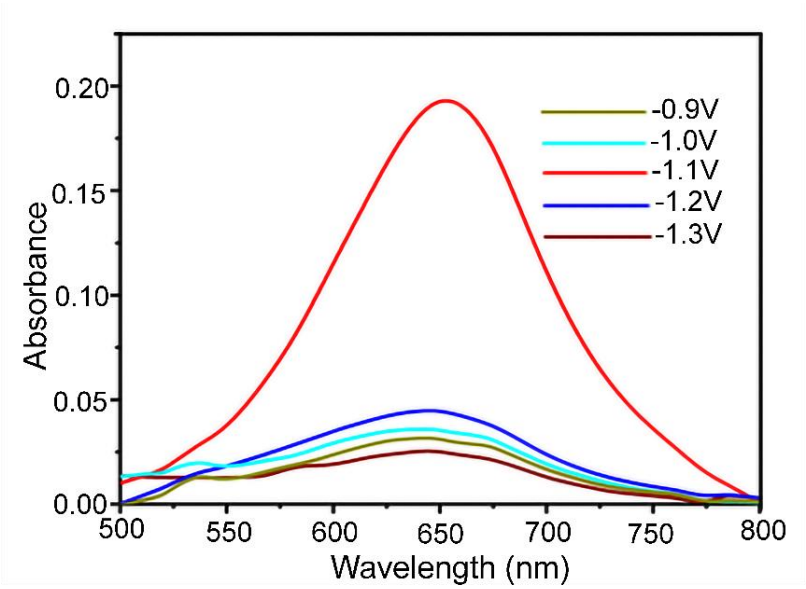

Fig. S7 UV-visible absorption spectra using graphene-oxide-supported Cu_6 NCs for NRR at corresponding potentials after 2 hours incubation using indophenol assay.

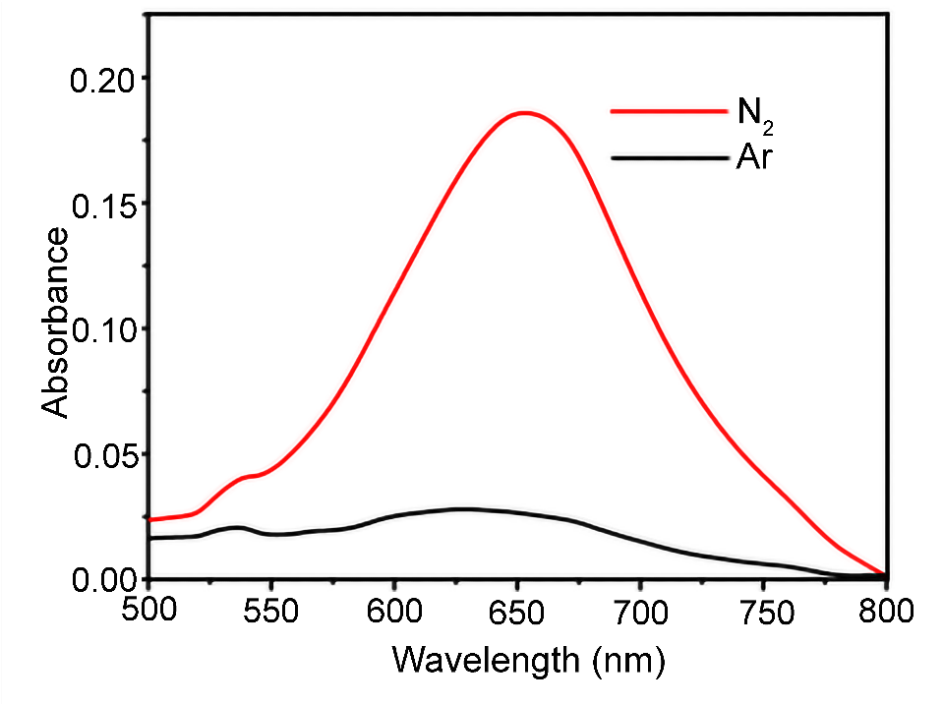

Fig. S8 UV-visible absorption spectra after NRR using graphene oxide supported Cu_6 NCs in N_2 and Ar-saturated environment at -1.1 V to confirm source of ammonia.

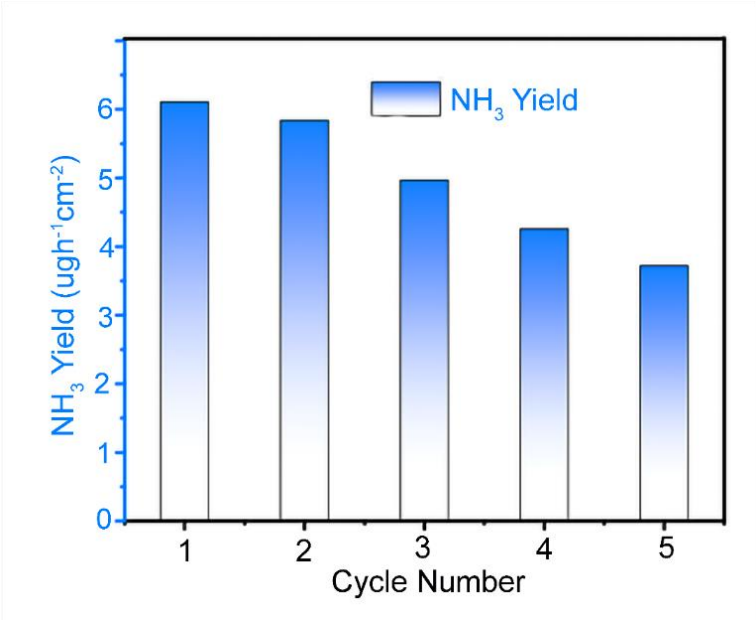

Fig. S9 NH_3 yields at -1.1 V versus RHE during recycling test for five times.

S3. Theoretical Calculation Details

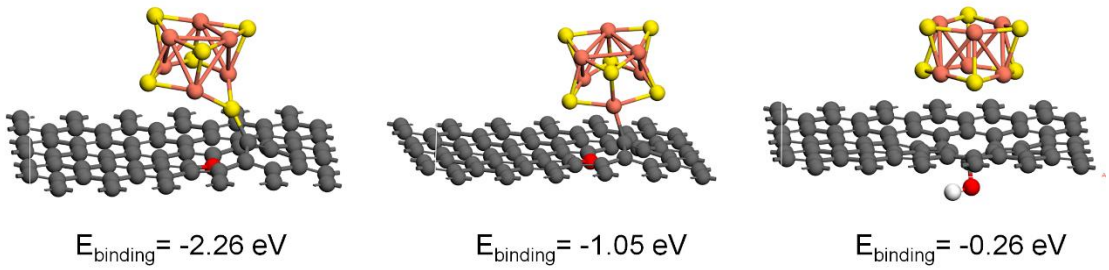

Fig. S10 Optimized structures of Cu_6 clusters supported on graphene oxide substrates.

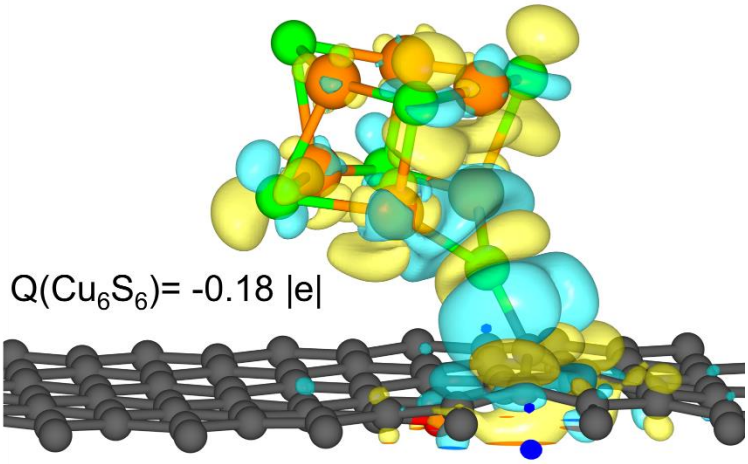

Fig. S11 The charge density difference of the Cu_6S_6 supported on GO.

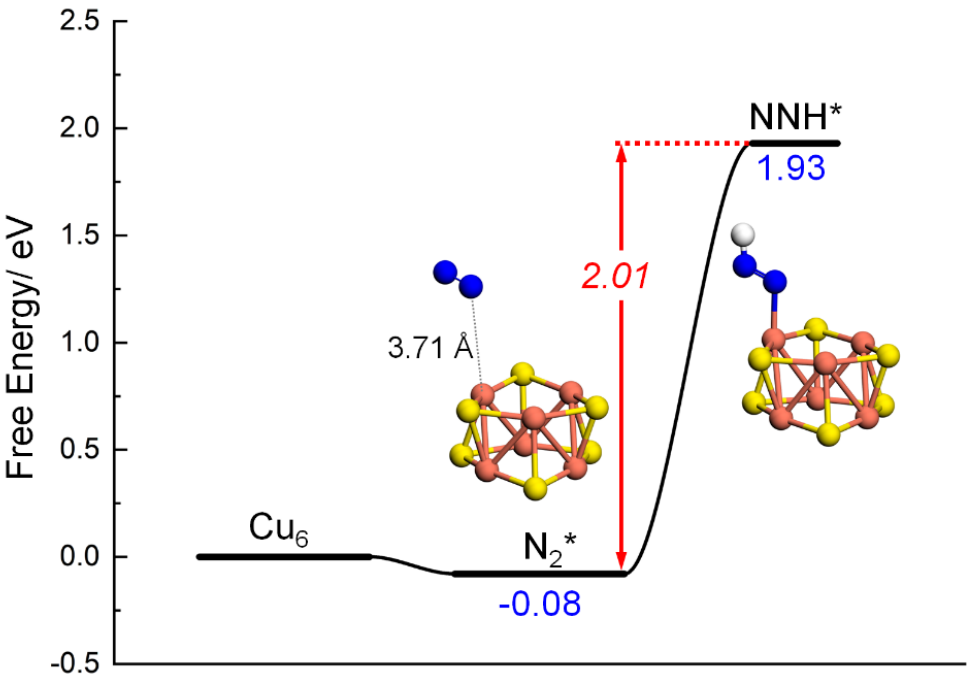

Fig. S12 Reaction pathway for N_2 adsorption and hydrogenation on a Cu_6S_6 cluster.

Table S1 Crystallographic data for the $Cu_6(SMPP)_6$ nanocluster

	In this work	In Ref.[2]
Empirical formula	$C_{42}H_{54}Cu_6N_{12}S_6$	$C_{44}H_{58.02}Cl_{4.03}Cu_6N_{12}S_6$
Formula weight	1300.57	1471.33
Temperature (K)	170.0(4)	293(2)
Crystal system	monoclinic	triclinic
Space group	P 2_1/n	P-1
a (Å)	11.88670(14)	9.2167(4)
b (Å)	13.06844(17)	13.7793(6)
c (Å)	16.4807(2)	23.2892(7)
α (deg)	90	78.740(3)
β (deg)	99.397	88.981(3)
γ (deg)	90	86.659(3)
Volume ($Å^3$)	2525.76	2895.81(19)
Z	2	2
ρ_{calc} (g/cm^3)	1.710	1.687
μ (mm^{-1})	5.425	2.609
F(000)	1320	1489.0
Crystal size (mm^3)	0.21 × 0.15 × 0.12	0.22 x 0.16 x 0.15
2Θ range for data collection (deg)	8.546 to 154.97	6.852 to 61.668
Index ranges	$-13 \le h \le 14$, $-12 \le k \le 16$, $-20 \le l \le 20$	$-11 \le h \le 13$, $-19 \le k \le 19$, $-33 \le l \le 33$
Reflections collected	16989	50454
Independent reflections	5169 [R_{int} = 0.0451, R_{sigma} = 0.0432]	16012 [R_{int} = 0.0459, R_{sigma} = 0.0576]
Data / restraints / parameters	5169/0/302	16012/327/733
Goodness-of-fit on F^2	1.053	1.150
Final R indexes [I>=2σ (I)]	R_1 = 0.0322, wR_2 = 0.0852	R_1 = 0.1189, wR_2 = 0.3059
Final R indexes [all data]	R_1 = 0.0364, wR_2 = 0.0885	R_1 = 0.1457, wR_2 = 0.3213
Largest diff. peak/hole (e $Å^{-3}$)	0.46/-0.42	3.78/-1.46

Table S2 Calculated bond lengths in synthesized Cu_6 nanoclusters

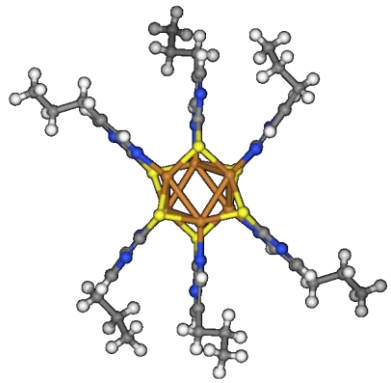

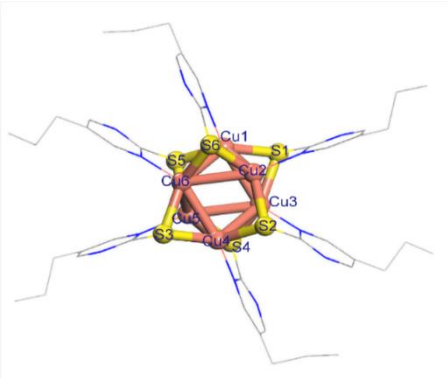

Sr. No	Bond	Bond length (Å)
1	Cu_1-Cu_2	2.689
2	Cu_2-Cu_3	2.909
3	Cu_3-Cu_4	2.877
4	Cu_4-Cu_5	2.689
5	Cu_5-Cu_6	2.909
6	Cu_6-Cu_1	2.877
7	Cu_1-S_1	2.230
8	Cu_3-S_1	2.247
9	Cu_2-S_2	2.270
10	Cu_4-S_2	2.278
11	Cu_4-S_3	2.230
12	Cu_5-S_3	2.247
13	Cu_3-S_4	2.263
14	Cu_6-S_4	2.244
15	Cu_5-S_5	2.270
16	Cu_1-S_5	2.278
17	Cu_2-S_6	2.244
18	Cu_5-S_6	2.263
19	Cu_1-N_1	2.041
20	Cu_2-N_2	2.044
21	Cu_3-N_3	2.049
22	Cu_4-N_4	2.041
23	Cu_5-N_5	2.049
24	Cu_6-N_6	2.044

Table S3 Comparison of NRR performance of Cu_6/GO with other electrocatalysts

Catalyst	Electrolyte	NH_3 yield	FE(%)	Ref.
Cu_6/GO NCs	0.1 M KOH	**4.8 μg·h^{-1}cm^{-2}**	**30.39**	This work
Cu NPs on Ti_3C_2	0.1 M KOH	3.04 μmol·h^{-1}cm^{-2}	7.31	3
TiO_2-rGO	0.1 M Na_2SO_4	15.13 μg·h^{-1}mg$^{-1}_{cat.}$	3.3	4
Au nanorods	0.1 M KOH	1.6 μg·h^{-1}cm^{-2}	3.88	5
β-FeOOH nanorod	0.5 M $LiClO_4$	23.32 μg·h^{-1}mg$^{-1}_{cat.}$	6.7	6
γ-Fe_2O_3	0.1 M KOH	0.212 μg·h-mg$^{-1}_{cat.}$	1.9	7
$Pd_{0.2}Cu_{0.8}$/rGO	0.1 M KOH	2.8 μg·h^{-1}mg$^{-1}_{cat.}$	4.5	8
MoS_2/CC	0.1 M Na_2SO_4	4.94 μg·h^{-1}cm^{-2}	1.17	9
Fe_3O_4/Ti	0.1 M Na_2SO_4	3.42 μg·h^{-1}cm^{-2}	2.6	10
TiO_2 nanosheets	0.1 M Na_2SO_4	5.6 μg·h^{-1}cm^{-2}	2.5	11
B-TiO_2	0.1 M Na_2SO_4	14.4 μg·h^{-1}mg$^{-1}_{cat.}$	3.4	12
MnB_x (NO_3 to NH_3)	0.1 M Li_2SO_4	74.9 ± 2.1 μg·h^{-1}mg$^{-1}_{cat.}$	38.5 ± 2.7	13
CoO/CuO-NA/CF (NO_3^- to NH_3)	0.5 M NaOH	296.9 μmol·h^{-1}·cm^{-2}	92.9	14
Au NCs on TiO_2 (NO_3^- to NH_3)	0.2 M Na_2SO_4 & 0.05 M $NaNO_3$	1923 μg·h^{-1}·mg$^{-1}_{cat.}$	91	15
Pd/TiO_2, (NO_3^- to NH_3)	0.1 M K_2SO_4	8.3 nmol·s^{-1}·cm^{-2}	25.6	16
Ru−O−V pyramid electron bridge	0.1 M Na_2SO_4	115 μg·h^{-1}·mg$^{-1}_{cat.}$	51.48	17
Bi-doped FeS_2 (NO_3^- to NH_3)	0.1 M KOH (H-cell)	21.9 μg·h^{-1}·cm^{-2}	98.5	18

References

1. G. W. Watt and J. D. Chrisp, *Anal. Chem.*, 1952, **24**, 2006−2008.
2. H. Wu, R. Anumula, G. N. N. Andrew and Z. Luo, *Nanoscale*, 2023, **15**, 4137−4142.
3. A. Liu, X. Liang, Q. Yang, X. Ren, M. Gao, Y. Yang and T. Ma, *ChemPlusChem*, 2021, **86**, 166–170.
4. X. Zhang, Q. Liu, X. Shi, A. M. Asiri, Y. Luo, X. Sun and T. Li, *J. Mater. Chem. A*, 2018, **6**, 17303–17306.
5. D. Bao, Q. Zhang, F.-L. Meng, H.-X. Zhong, M.-M. Shi, Y. Zhang, J.-M. Yan, Q. Jiang and X.-B. Zhang, *Adv. Mater. (Weinheim, Ger.)*, 2017, **29**, 1604799.
6. X. Zhu, Z. Liu, Q. Liu, Y. Luo, X. Shi, A. M. Asiri, Y. Wu and X. Sun, *Chem. Commun.*, 2018, **54**, 11332–11335.
7. J. Kong, A. Lim, C. Yoon, J. H. Jang, H. C. Ham, J. Han, S. Nam, D. Kim, Y.-E. Sung, J. Choi and H. S. Park, *ACS Sustain. Chem. Eng.*, 2017, **5**, 10986−10995.
8. M.-M. Shi, D. Bao, S.-J. Li, B.-R. Wulan, J.-M. Yan and Q. Jiang, *Adv. Energy Mater.*, 2018, **8**, 1800124.
9. L. Zhang, X. Ji, X. Ren, Y. Ma, X. Shi, Z. Tian, A. M. Asiri, L. Chen, B. Tang and X. Sun, *Adv Mater*, 2018, **30**, e1800191.
10. Q. Liu, X. Zhang, B. Zhang, Y. Luo, G. Cui, F. Xie and X. Sun, *Nanoscale*, 2018, **10**, 14386–14389.
11. R. Zhang, X. Ren, X. Shi, F. Xie, B. Zheng, X. Guo and X. Sun, *ACS Appl. Mater.*

Interfaces, 2018, **10**, 28251−28255.
12. Y. Wang, K. Jia, Q. Pan, Y. Xu, Q. Liu, G. Cui, X. Guo and X. Sun, *ACS Sustain. Chem. Eng.*, 2019, **7**, 117−122.
13. M. A. Mushtaq, A. Kumar, W. Liu, Q. Ji, Y. Deng, G. Yasin, A. Saad, W. Raza, J. Zhao, S. Ajmal, Y. Wu, M. Ahmad, N. U. R. Lashari, Y. Wang, T. Li, S. Sun, D. Zheng, Y. Luo, X. Cai and X. Sun, *Adv Mater*, 2024, **36**, e2313086.
14. S. Chen, G. Qi, R. Yin, Q. Liu, L. Feng, X. Feng, G. Hu, J. Luo, X. Liu and W. Liu, *Nanoscale*, 2023, **15**, 19577–19585.
15. M. Yang, T. Wei, J. He, Q. Liu, L. Feng, H. Li, J. Luo and X. Liu, *Nano Res.*, 2024, **17**, 1209–1216.
16. K. Dong, Y. Yao, H. Li, H. Li, S. Sun, X. He, Y. Wang, Y. Luo, D. Zheng, Q. Liu, Q. Li, D. Ma, X. Sun and B. Tang, *Nat. Synth.*, 2024, **3**, 763–773.
17. Y. Sun, X. Li, Z. Wang, L. Jiang, B. Mei, W. Fan, J. Wang, J. Zhu and J. M. Lee, *J. Am. Chem. Soc.*, 2024, **146**, 7752–7762.
18. G. Zhang, G. Wang, Y. Wan, X. Liu and K. Chu, *ACS Nano*, 2023, **17**, 21328–21336.